Moving-Coil Loudspeaker Topology as an Indicator of Linear Excursion Capability*

MARK R. GANDER

James B. Lansing Sound, Inc., Northridge, CA 91329, USA

The knowledge of a loudspeaker structure's physical dimensions and features can directly predict both the maximum excursion before damage and the linear excursion limit as defined by psychoacoustic or performance criteria. Various voice-coil, magnetic-gap, and suspension configurations are discussed in terms of their potentials for linear motion. Measurements which substantiate the predicted linearity are presented, and specific structures and mechanisms which extend or degrade the predicted linearity are also discussed.

0 INTRODUCTION

To make sound, you must move air. The most common and popular electroacoustical method of sound production involves exciting the air with the motion of a diaphragm, which is driven by an ac modulated electrical signal controlling a moving-coil permanent magnet motor structure. The motion of this diaphragm–motor assembly must be linear if the resulting sound output is to be linear, that is, distortion free. The reproduction of sound at low frequencies and high levels requires the generation of considerable volume velocities, and the finite dimensions of the diaphragm and motor components limit first the ultimate excursion capability before damage, and further the excursion for some chosen acceptable or allowable level of nonlinearity. By examining the topology (the basic layout and physical features) of various types of loudspeakers, inferences can be made as to their individual performance and characteristics, and predictions made as to their relative and absolute linearity.

1 EXCURSION LINEARITY CRITERIA

It is important to know the excursion capability of a given transducer in order to determine its suitability for the intended application. Knowing both the maximum

excursion and the thermal power input rating, the maximum sound output can be determined. The regions of thermal and excursion limitation can be determined for various enclosure and system alignments. From these predictions the suitability of the transducer for various applications and systems can be determined.

Before we can judge an individual transducer for excursion capability, we must determine what criteria we will use to make this judgment. The absolute maximum excursion is the physical limit of diaphragm motion as defined by the mechanical structure of the device in question. This defines the maximum excursion limits before damage, or the "maximum throw" of a driver, which is occasionally quoted by manufacturers if any mention of excursion capability is made at all. This information is not without use, for the obvious reason of preventing driver damage and also in applications where only sound output and not sound quality is desired. In most cases, however, we are interested in the extent of motion that the device can undergo within some linearity constraint.

Most authors discuss the motional linearity of loudspeakers only in the general terms of requiring larger magnet and coil structures [1, pp. 195, 252–253; 2, p. 262]. Thiele defines x_{max} as a peak displacement limit, but assigns no criteria for its determination although he derives various formulas using peak displacement values [3, pp. 472–473]. Small has done the most extensive work on displacement-limited power ratings for trans-

ducers [4, pp. 391–393] and suggests that the amount of voice-coil overhang be used as a rough estimate of driver linearity [5, p. 806]. This does not address voice-coil/ magnetic gap topologies other than the overhanging coil, and neglects the effects of fringe flux outside the magnetic gap, which are significant.

2 NONLINEARITY GENERATING HARMONIC COMPONENTS

Olson has analyzed the effects of nonlinear elements in producing harmonic distortion components [6]. He has shown that for a force as a function of displacement of the form

$$F(x) = ax + bx^3 \tag{1}$$

Fourier analysis will yield solutions of the form

$$x = A \cos \omega t + B \cos 3\omega t. \tag{2}$$

This is the form taken by balanced, or symmetric, non-linearity, where the distortion manifests itself as a third-harmonic term. For a force-displacement function of the form

$$F(x) = ax + bx^2 \tag{3}$$

the solution yields

$$x = A \cos \omega t + B \cos 2\omega t \tag{4}$$

which shows the presence of second-harmonic distortion. In this case we are dealing with single-ended non-linearities.

Typical loudspeakers can be seen to have a force function with both square and cubic terms. The cubic terms are manifested as the coil is driven out of the magnetic field to an equal extent on both sides of the gap, a symmetric nonlinearity yielding third-harmonic distortion. Thus we would expect our linear excursion limit to manifest itself purely in terms of third-harmonic distortion. The square terms can come about if the gap flux and fringe are nonsymmetrical, if the coil rest position is not centered in the magnetic gap, or if rectification or other effects impart a dc offset to the coil travel midpoint under drive. Any of these effects will produce a single-ended nonlinearity, giving second-harmonic distortion. It should be noted that the driver should be inherently free of second-harmonic distortion, only exhibiting third-harmonic distortion due to finite coil and gap heights. In both cases, higher order terms have been left out of the analysis due to their much lower amplitudes compared to the second- and third-harmonic components.

3 VOICE-COIL/MAGNETIC-GAP CONFIGURATIONS AND FLUX DISTRIBUTIONS

Fig. 1 shows views of the three types of voice-coil/ magnetic-gap configurations in cross section. They are the long coil–short gap or overhung coil; the long gap–short coil or underhung coil; and the equal-length coil

and gap. Here they are sketched with symmetrical gap geometries, but this is not always the case. Often there is only a single slug center pole, as in Fig. 2, instead of a separate protruding pole piece resting on a pole support with a smaller outside diameter. The top plate support, be it a magnet or á metal magnetic circuit return casing, may have its inside diameter only slightly larger than that of the top plate. The exact configuration of the magnetic gap becomes important because the magnetic flux is never confined strictly to the gap, but spreads out forming fringe lines above and below the gap. If the permeance of the region below the gap is higher than that above due to the presence of magnetic structure elements too near the gap, more lines of fringe flux will exist below the gap than above. This will cause the coil to move in a nonsymmetrical flux field and hence cause distortion. Even in a symmetrical magnetic gap, fringe lines are inevitable and can at best be made even on both sides of the gap (Fig. 3). Various other symmetrical gap geometries which attempt to equalize fringe flux, such as extended center poles and chamfered gap tips, have also been utilized [7, pp. 239–241].
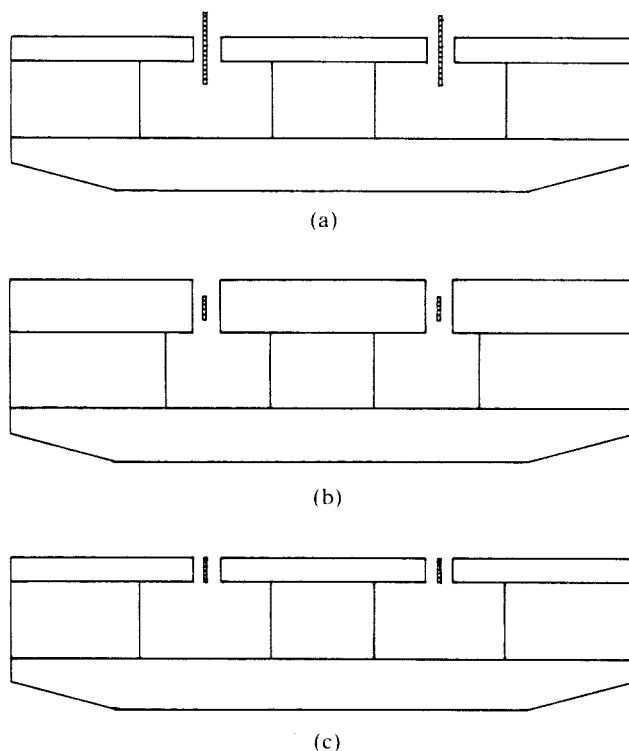

(a)

(b)

(c)

Fig. 1. The three basic voice-coil/magnetic–gap configurations. (a) Overhanging coil. (b) Underhung coil. (c) Equal-length coil and gap.
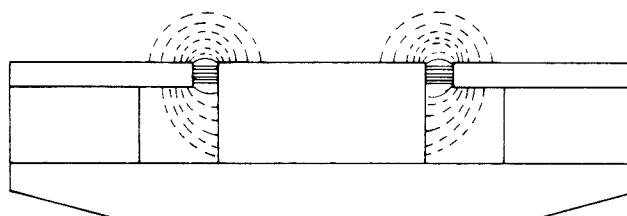

Fig. 2. Flux distribution in nonsymmetrical gap showing uneven fringe field.

The presence of fringe flux is an important key to the understanding of loudspeaker linearity. Fig. 4 shows typical flux distributions for various gap configurations. Fig. 4(a) is the theoretical ideal, where all the lines are concentrated evenly within the gap and no flux is present outside. Fig. 4(b) represents the best that is practically attainable, with even distribution across most of the gap, which begins to reduce as the gap edges are approached and gradually approaches zero as the fringe flux weakens away from the gap. If the gap is at all nonsymmetrical, the flux distribution will take a form similar to Fig. 4(c). Here the fringe flux is significantly greater in the inward direction. For wide gaps the flux within the gap can also be affected.

For a coil moving in a flux field, the Bl product is proportional to the total flux passing through the surface ara of the coil. Bl will change if the total number of lines of flux through the coil area changes. For underhung and equal-length topologies this occurs as one end of the coil begins to leave the gap. For overhung coils, where the fringe flux is a significant portion of the total flux at rest position, this will begin to occur as soon as there is any coil motion. The degree of change depends on the specific spatial distribution of the fringe flux field, but definitely becomes dominant as the end of the coil approaches and enters the gap.

4 MOTOR FORCE

For the diaphragm to be capable of linear excursions, the loudspeaker must provide linear diaphragm motion relative to the electrical input signal. The force provided by the motor is the product of current I, which is the input signal, and the Bl product, the motor strength:

$$F = (Bl)I. \tag{5}$$

The input signal is here a current, but in almost all applications we drive loudspeakers from constant voltage source amplifiers. For an input voltage E, the current I is given by

$$I = \frac{E}{Z_{cc} + Z_{cm}} \tag{6}$$

where Z_{cc} is the blocked electrical impedance consisting of the dc resistance and voice-coil inductance, and Z_{cm} is the electrical motional impedance generated by the back EMF of the coil motion. This electrical motional impedance is given by

$$Z_{cm} = \frac{(Bl)^2}{Z_{mt}} \tag{7}$$

where Z_{mt} is the total mechanical impedance, including the radiation impedance due to the air load on the moving diaphragm.

Combining Eqs. (6) and (7) into Eq. (5),

$$F = \frac{(Bl)E}{Z_{cc} + (Bl)^2/Z_{mt}}. \tag{8}$$

In the region of resonance $Z_{cm} \gg Z_{cc}$, so that

$$F = \frac{E Z_{mt}}{Bl} \tag{9}$$

and the force is inversely proportional to Bl. Here we have the surprising result that as the Bl decreases, the motor force actually increases. The increased force will continue until the decrease in Bl causes the motional impedance to no longer be dominant over the blocked electrical impedance. The force will then decrease from its maximum value to zero, passing through a point of full linearity along the way. Under most operating conditions, loudspeakers are required to undergo maximum excursion in the region of resonance and are subject to this effect. It will also vary with the acoustic loading of the driver, since the motional impedance will change frequency and shape in sealed, vented, and horn-loaded enclosures.

Another distortion mechanism is an offset in the coil rest position. Any difference in the coil rest position from the position of maximum Bl will cause second-harmonic distortion. This can come about due to improper physical construction, gravity bias depending on the axial orientation of the unit, dc present in the drive signal, or a nonsymmetrical flux field, as already discussed.

A solenoidal force is generated between the voice coil and the center pole, produced by the change in voice-coil inductance both with coil position and with change in saturation level of the center pole [8], [9]. This causes a force creating a dc offset causing second-harmonic distortion.

An offset in the coil rest position can also be imparted due to dynamic instability, the electromechanical rectification effect first described by McLachlan [7, pp. 245–251]. This is another artifact of the variation of
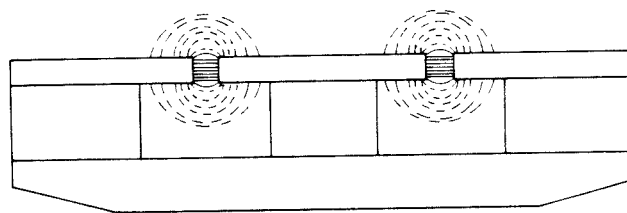

Fig. 3. Flux distribution with symmetrical field geometry showing equal fringe field on both sides of gap.
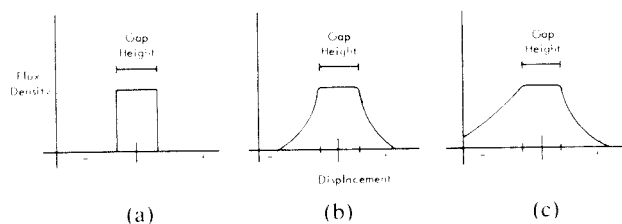

Fig. 4. Flux distribution with displacement along axial length of magnet structure. (a) Ideal field. (b) Symmetrical field geometry. (c) Nonsymmetrical gap geometry.

motor force with displacement caused by the fringe field, where the coil rest position will actually jump in or out to the suspension limit. In the mass-controlled region above resonance the coil acceleration is 180° out of phase with the displacement. If the input level is large enough to exceed the expansion region, where *Bl* decreases cause motor force increases, both the acceleration and the current will be minimum at the extremes of coil travel. The coil will tend to jump toward this weaker field [10]. This will cause a distinct rise in distortion due to the offset in the region from resonance up to 150 Hz or so, where the amplitude is no longer sufficient to cause jump-out. This effect is prevalent in long coil–short gap loudspeakers, and usually will not occur in underhung coil structures since their coil motion is within a linear flux field.

5 SUSPENSION FORCE

The use of nonlinear or progressive suspensions can prevent or reduce these distortion mechanisms. Harwood noted the fact of increasing motor force from the linear level before the decrease, and showed how a loudspeaker could be fitted with a suspension which increased its stiffness force at the correct rate to compensate for the increased motor force, thus increasing the linearity of the system [11]. This is so because the other dominant force in the system is that provided by the stiffness of the suspension elements at the instantaneous excursion. Olson has shown that nonlinear suspensions can be approximated by the addition of a cubic term, the same mathematical order as the motor force nonlinearity [12]. The stiffness, the *Bl* product, and the suspension losses all vary with displacement. For displacements where the motor force factors remain approximately constant and much greater than the suspension force nonlinearities, the total driving force will be relatively linear. In all other cases the variations in these elements will determine the force function, and if the nonlinear components are in balance, the net force linearity can actually be extended. The nonlinearity of the suspension force can be made sufficiently strong to overcome the dc components of the motor force, but insignificant compared to the ac motor force, preventing dc offset [13].

Typical progressive suspension elements are those with high nominal stiffness, such as treated one-piece cone edges and cloth rolls impregnated with phenolic resin or other damping chemicals. Centering spiders also contribute to the stiffness characteristics. These are usually made of treated cloth in a flat disk or cup shape with corrugations to provide increased nominal compliance and linearity, the exact characteristics being determined by the shape of the corrugations, the thickness of the material, and the degree of treat. Half-roll surrounds of foam or rubber are usually of very low stiffness, but even loudspeakers fitted with these can exhibit progressive stiffness at long excursion if their limits are reached. Conversely, if the suspension force increases at too great a rate, it may exceed the motor force and limit linearity.

6 OTHER FEATURES AFFECTING LINEARITY

Voice-coil/magnetic-gap dimensions primarily determine linearity in the stiffness and resistance controlled regions, below approximately 150 Hz for most low-frequency loudspeakers. In the mass-controlled region of operation venting effects in the motor structure and magnetic field nonlinearities tend to dominate the distortion characteristics up to and slightly beyond the piston-band limit, where cone breakup distortions are the major source of nonlinearities.

Venting of the loudspeaker structure is usually associated with heat dissipation and power-handling considerations, but it is also necessary to prevent nonlinearity of the air from causing distortion. Methods employed to eliminate this problem include a porous or perforated center dome, voice-coil former perforations, or a vent hole through the center of the magnet structure [14, pp. 297–298]. A vent in the rear of the magnet structure must have sufficient area to prevent turbulent nonlinearity, and must be partially blocked with open-cell foam or screen to prevent foreign particles from entering the magnetic gap.

The magnetic field itself can undergo modulation due to the ac field generated by the current in the voice coil. This effect was first identified by Cunningham [8] and more fully investigated by Gilliom [15], and creates second-harmonic distortion proportional to coil current. This effect manifests itself most when the center pole within the coil is constructed to high-permeance material, so that motors with center poles operated at a saturated flux level, or centrally placed Alnico magnets, are relatively immune. Fig. 5 illustrates some of the various methods which can be employed to eliminate this source of distortion, all involving the use of a shorted turn or Faraday loop within the magnet structure
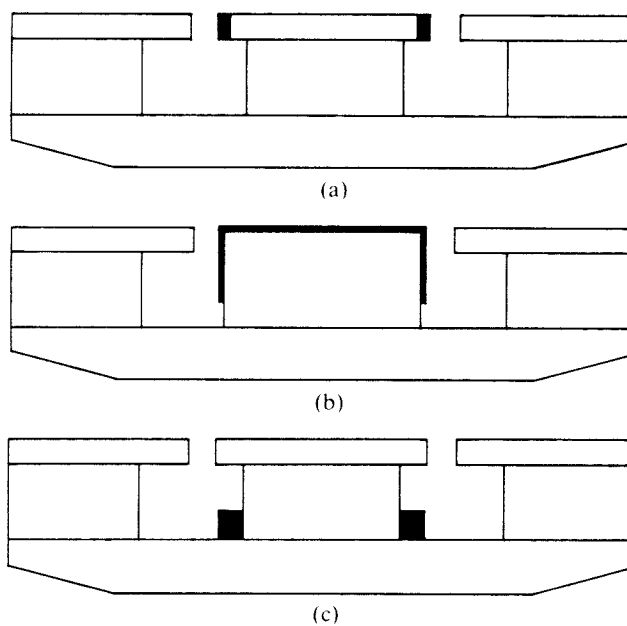

(a)

(b)

(c)

Fig. 5. Methods of providing a shorted turn within the magnetic field to prevent modulation by the voice-coil current. (a) Conductive plating on pole tips. (b) Conductive cap over pole piece. (c) Conductive ring.

which acts to generate a field equal and opposite to any changing field induced by the voice coil. A conductive ring can be placed around the center pole, a conductive cap can be placed over the pole piece, or a ring of conductive plating may be applied to the pole tips. If the conductive ring is placed in the gap, the effective gap size and hence gap reluctance is increased, increasing the fringe field and requiring a larger magnet for the same gap flux. The pole piece cap also precludes symmetric gap geometry, making the flux field unsymmetrical as well. If conductive rings are used anywhere within the coil, they will tend to reduce the voice coil inductance rise at high frequencies and hence increase acoustic output. This effect may or may not be desirable, although in some cases it is the only motivation for using the ring, not for its distortion-reducing characteristics [16]. If the conductive ring is located around the center pole, care must be taken in the placement and size of the ring to prevent large changes of voice-coil inductance with the position. In addition to causing second-harmonic distortion from the solenoidal force, this effect can cause modulation of high-frequency tones by large low-frequency excursions, a serious performance detriment and a linearity criterion in itself [17].

The presence of conductive rings directly within the gap may also tend to reduce third-harmonic distortion generated due to the magnetization of the magnetic gap pole surfaces by the voice-coil flux. This particular problem can be attacked directly by constructing the pole surfaces from material with a very linear magnetization characteristic. This method has no effect on flux modulation of the permanent field, however, and hence does not reduce second-harmonic distortion.

7 APPROXIMATE LINEARITY PREDICTION

From this analysis we can formulate predictions for the linearity of the three basic types of loudspeaker motors. If the height of the coil and the magnetic gap are known, the peak displacement of the unit should be approximately given by half the magnitude of the difference of these two dimensions plus a correction factor for fringe effects. For overhung coils the coil may move past the fringe field on one side and just begin to enter the gap before gross nonlinearity occurs. The correction factor is therefore zero for this topology, and the formula is the same as that suggested by Small [5, p. 806]:

$$x_{max} = \frac{\text{voice-coil height} - \text{gap height}}{2}. \quad (10)$$

Equal and underhung units may have their coils leave the gap by some percentage approximating the fringe field on each side of the gap before gross distortion occurs, effectively lengthening the gap and increasing linearity. If a 15% factor is adopted as an approximation for the fringe field extension on each side of the gap, then the formula becomes for underhung and equal coil and gap topologies:

$$x_{max} = \frac{\text{gap height} - \text{voice-coil height}}{2}$$

$$+ 15\% \text{ (voice-coil height)}. \quad (11)$$

While only direct measurement of the Bl product and the suspension stiffness values with displacement can accurately predict the exact linearity for a given unit, these formulas should provide a good approximation in the absence of further data. A given unit will have to be inspected for clues as to whether its linearity may be increased due to the balancing of motor and suspension nonlinearities, or decreased due to dc offset effects or excessively stiff suspension elements.

8 CHOICE OF LINEARITY LIMIT

The assignment of a linearity limit presents a problem because a definition of acceptable linearity must be chosen. The desired or required linearity will depend on the quality requirements of the particular application. For most sound production and reproduction uses, the question of assigning a number moves from the realm of engineering acoustics to psychoacoustics. When we talk of the linearity of reproduced sound we are talking about distortion. Noticeable, acceptable, and tolerable levels of distortion vary with both frequency and the level of the sound being produced, the content of the sound, whether the signals are transient or steady state in nature, as well as the quality of the listener.

Probably the most common method of assessing the linearity of a given transducer is an "eyeball–earball" test, driving the device near resonance and increasing the input until it begins to "sound bad," and measuring the displacement at this level, an arbitrary process at best. Small suggests the criterion of driving the loudspeaker at resonance in free air and measuring the displacement at 10% total harmonic distortion [5, p. 806]. These methods assume no variation of excursion linearity with frequency and drive level, which can be substantial for certain topologies.

A 3% distortion level seems a more appropriate choice for the linearity limit. Measurements on various types of transducers indicate a good correlation of the peak piston displacement for this distortion level with the predicted maximum linear displacement. A 3% (−30 dB) distortion component relative to the fundamental contributes less than ¼ dB to the total acoustic output, so that maximum sound pressure level calculations will not be seriously affected [4, p. 393]. The peak-to-average ratio in most program material is quite high, and the signal material is usually transient in nature. These and other factors indicate that under program conditions with a system designed with this level of peak displacement in mind, the 3% distortion level will only be reached occasionally, and then psychoacoustic factors should tend to mask the full negative effects of such distortion. We would like to think that distortions below 1% are possible as the chosen criterion, but these types of figures will in general lead to unusually conservative linearity figures. At an input level approaching the thermal input capabilities of the loudspeaker, other distortions associated with but not directly related to the motional linearity will also be increasing, such as cone breakup

and electrical, thermal, and magnetic field effects. The choice of a 3% distortion limit on any and all distortion products seems to be an appropriate compromise between the maximum excursion before damage and some arbitrarily low distortion level. Adequate headroom will normally be built in, as with any intelligent design, so that this level will not often be reached. For those applications involving sustained high-output low-frequency tones, and for ultimate quality requirements, both the maximum excursion and the maximum input power should be scaled down accordingly.

9 EXCURSION MEASUREMENT METHODS

Various methods have been employed to measure diaphragm displacements. The destructive excursion limit can be algebraically computed from structural dimensions or directly measured by physical displacement of the moving assembly, inward until the bottom of the coil form hits the back of the structure and outward until the coil form leaves the gap, or until the suspension elements allow no more motion. The assignment of a linear limit poses a more difficult problem in that the excursion must be measured under sinusoidal excitation varying with frequency and amplitude. Direct visual measurement, displacement probe, laser [18], and accelerometer [19] techniques have all been utilized. Data can be taken at constant amplitude input with varying frequency, and at constant frequency with increasing input. The results can be plotted directly and analyzed for linearity, or acoustic measurements may be taken simultaneously on the sound output, analyzed for distortion components, and compared with the excursion data. All these methods involve direct measurement of the displacement, but the displacement may be accurately computed from the acoustic measurements themselves.

10 PEAK PISTON DISPLACEMENT

The axial sound intensity output from a piston source operating into one side of an infinite baffle is given by [2, p. 175]

$$I = 2\rho_0 c u^2 \sin^2\left[\frac{k}{2}(\sqrt{r^2 + a^2} - r)\right] \qquad (12)$$

where

I = intensity magnitude
ρ_0 = density of air, 1.21 kg/m at 20°C
c = velocity of sound in air, 343 m/s
u = peak piston velocity
k = wave number, $2\pi/\lambda = \omega/c$
r = distance from measuring point to center of piston
a = piston radius

For distances from the piston large compared to its radius, $r \gg a$, Eq. (12) can be shown to converge to

$$I = \frac{\rho_0 c k^2 a^4 u^2}{8r^2} . \qquad (13)$$

The intensity is related to the pressure by

$$I = \frac{p^2}{2\rho_0 c} . \qquad (14)$$

Combining Eqs. (13) and (14) and taking the square root, the pressure is given by

$$p = \frac{\rho_0 c k a^2 u}{2r} . \qquad (15)$$

Solving for the velocity u,

$$u = \frac{2rp}{\rho_0 c k a^2} . \qquad (16)$$

For sinusoidal excitation, the piston displacement can be represented as

$$x_0 = x \sin \omega t. \qquad (17)$$

The piston velocity u is the derivative with respect to time of the piston displacement:

$$u = \frac{dx_0}{dt} = \omega x \cos \omega t. \qquad (18)$$

Therefore the maximum peak diaphragm displacement is

$$x_{\text{peak}} = \frac{u}{\omega}. \qquad (19)$$

Substituting Eq. (16) into Eq. (19),

$$x_{\text{peak}} = \frac{rp}{2\rho_0 \pi^2 f^2 a^2} . \qquad (20)$$

Eq. (20) can be modified for the case of a 4π sr radiating field for measurement in anechoic environments by substituting a factor of 2 to account for the increase in the integrating area:

$$x_{\text{peak}} = \frac{rp}{\rho_0 \pi^2 f^2 a^2} . \qquad (21)$$

The stipulations are that $r \gg a$, that the measurement is performed in the far field of the transducer; and that $\lambda > 2\pi a$, that we are radiating omnidirectionally. This stipulates that we are in the piston band of the transducer.

Keele's work on near-field measurement also applies directly. His relationship between the near- and far-field pressures [20, Eq. (5), p. 155]

$$p_N = \frac{2r}{a} p_F \qquad (22)$$

can be substituted into Eq. (20), yielding

$$x_{\text{peak}} = \frac{p_N}{4\rho_0 \pi^2 f^2 a} . \qquad (23)$$

The near-field pressure can then indicate directly the

piston excursion, with all the appropriate caveats applied.

Instead of making a separate measurement, we can now make our normal acoustic sound pressure measurements and simultaneously know the excursion which the driver is undergoing. In particular we can make acoustic distortion measurements and correlate the levels of distortion and individual component contributions with the excursion.

11 EXPERIMENTAL MEASUREMENTS

Swept sine wave sound pressure amplitude versus frequency curves were taken on an outdoor ground platform with the measurement microphone directly above the test loudspeaker at a distance of 1 m on axis. The platform has no substantial obstructions for a distance of at least 15 m in all directions along the ground surface so as to effectively provide a half-space 2π sr measurement environment. The rear of the loudspeaker units were surrounded by a 280-liter well-braced enclosure extensively lined with damping material. The effective volume of the rear chamber was sufficient to have only minimal effect on even the most highly compliant of the units tested. Gravity bias is a potential problem in measurement environments such as this. The most highly compliant loudspeakers have stiffnesses on the order of 1.5×10^3 N/m, and for moving masses as large as 0.15 kg under a gravity acceleration of 9.8 m/s^2 the moving assembly displacement will be approximately 1 mm. Stiff suspension units show displacements of less than 0.2 mm. This bias is a single-ended nonlinearity affecting only second-harmonic distortion, and the third-harmonic displacement linearity should not be affected. A tracking filter was used to isolate the second- and third-harmonic components, which in all cases are raised 20 dB each for convenience.

For pressure in terms of dB sound pressure level,

$$p = \sqrt{2}\, p_{rms} \tag{24}$$

$$SPL = 20 \log \left(\frac{p_{rms}}{p_{ref}} \right) \tag{25}$$

$$p_{rms} = 10^{SPL/20}\, p_{ref} \tag{26}$$

where

$$p_{ref} = 20\mu \text{ N/m}^2.$$

Since all measurements are at 1 m, we can combine this and the other constants of Eq. (20), reducing it to the convenient form

$$x_{peak} = \frac{(1.18 \times 10^3)\, 10^{SPL/20}}{f^2 a^2} \tag{27}$$

where x_{peak} and a are in millimeters.

Data were taken at different voltages to show the effects of variations in drive levels, but as the formula indicates, neither the actual input power level nor the power transfer efficiency of the measured unit is of concern in determining the excursion.

Other than measurement accuracy in determining the sound pressure level at a given frequency, the only variable in question is the effective piston radius for the loudspeaker diaphragm, usually consisting of a rigid truncated cone and flexible outer surround. Strictly geometrical considerations show that this can be accurately given by the radius of the rigid part of the diaphragm plus one-half the width of the flexible surround.

An initial test can be performed to indicate the unit's susceptibility to dc shift and jumpout. The transducer can be driven at a frequency above resonance where the excursion will be significant and the input voltage increased to approach the thermal limit. A reference point on the moving assembly can be viewed relative to a stationary point on the frame, and any deviations from equal positive and negative increase noted.

Fig. 6 shows the response of a 300-mm (128-mm effective piston radius) loudspeaker with an equal coil and gap height of 7.2 mm being driven by 9 V rms (8 Ω nominal impedance). The suggested formula for linearity predicts

$$x_{max} = \frac{7.2 - 7.2}{2} + 0.15\,(7.2) = 1.1 \text{ mm}. \tag{28}$$

If we choose the point where the third-harmonic distortion reaches 3.16% (−30 dB), here where the fundamental and third-harmonic curves are 10 dB apart since the distortion curves are raised 20 dB, the excursion that the loudspeaker is undergoing at this distortion level is

$$x_{peak} = \frac{(1.18 \times 10^3)\, 10^{103/20}}{(105)^2\,(128)^2} = 0.9 \text{ mm} \tag{29}$$

which agrees very closely with the prediction. Fig. 7 shows another driver of the same type, but assembled with the coil not centered but riding approximately 1 mm high. As predicted, the second harmonic is greatly increased but the third harmonic remains at the same level:

$$x_{peak} = \frac{(1.18 \times 10^3)\, 10^{101/20}}{(88)^2\,(128)^2} = 1.0 \text{ mm}. \tag{30}$$

Fig. 8 shows the response of a 380-mm (167-mm effective piston radius) driver with an underhung 7.2-mm coil in an 8.9-mm gap being driven by 13 V rms (16 Ω nominal impedance). The predicted linearity is

$$x_{max} = \frac{8.9 - 7.2}{2} + 0.15\,(7.2) = 1.9 \text{ mm}. \tag{31}$$

The −30 dB third-harmonic distortion point yields

$$x_{peak} = \frac{(1.18 \times 10^3)\, 10^{102/20}}{(58)^2\,(167)^2} = 1.6 \text{ mm}. \tag{32}$$

showing good agreement with prediction. When dealing with highly damped (low Q) drivers it is sometimes difficult to accurately determine distortion data due to
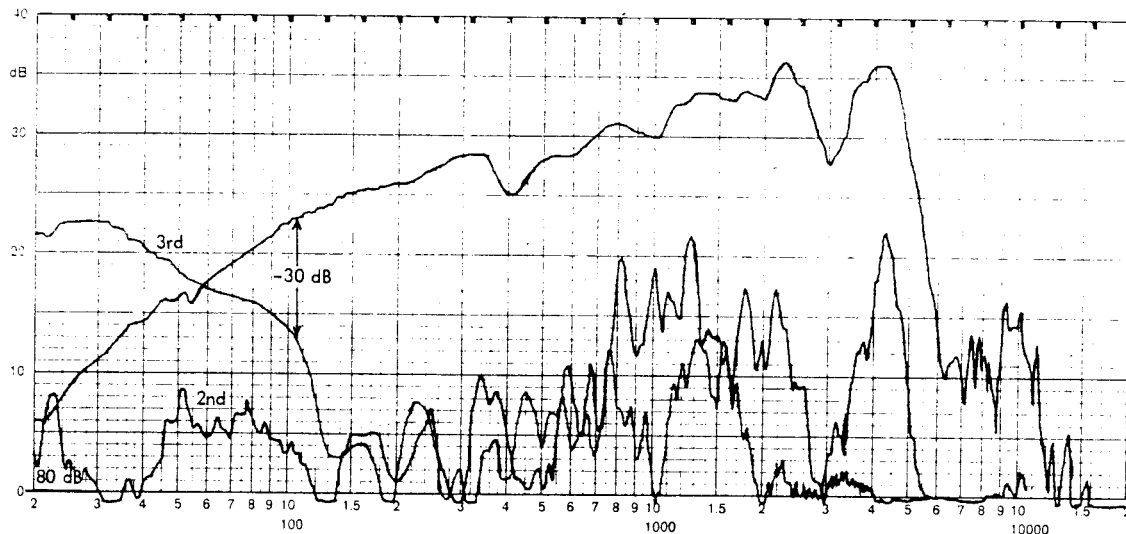
Fig. 6. Half-space on-axis amplitude response of a 300-mm (128-mm effective piston radius) loudspeaker with equal coil and gap height of 7.2 mm, 9 V rms input, 8 Ω nominal impedance. Distortion products raised 20 dB.
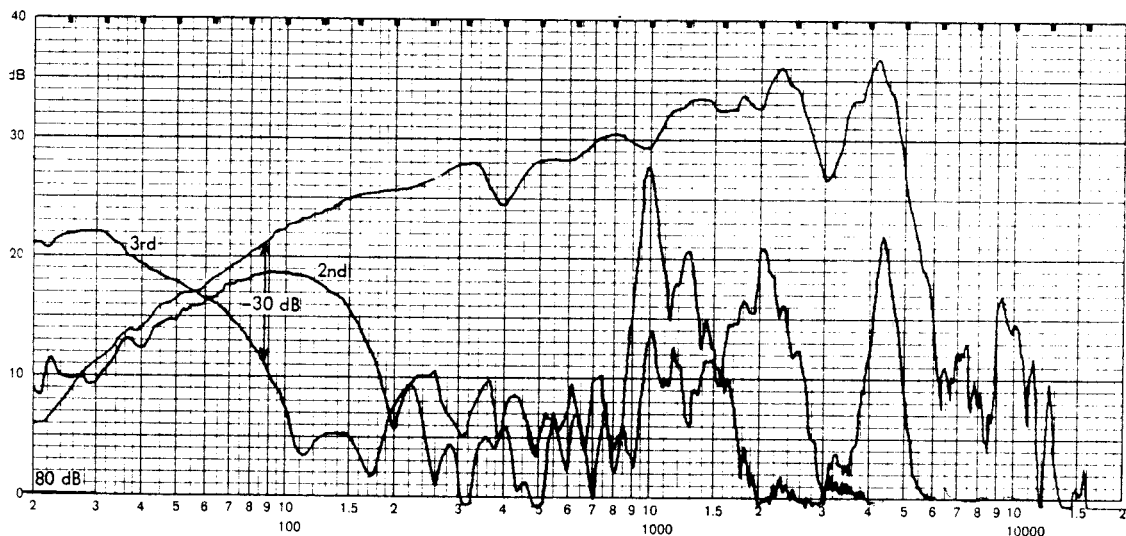

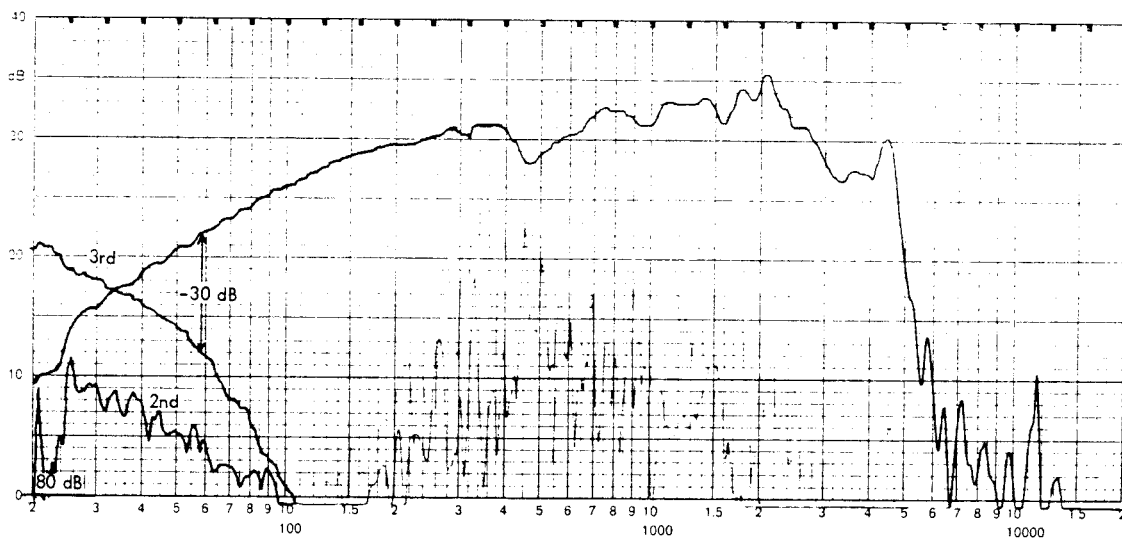Fig. 7. Same conditions as Fig. 6, but loudspeaker assembled with voice coil 1 mm off center.

Fig. 8. Half-space on-axis response of a 380-mm (167-mm effective piston radius) loudspeaker with a 7.2-mm coil in an 8.9-mm gap, 13 V rms input, 16 Ω nominal impedance. Distortion products raised 20 dB.

the skewed shape of the curves. If the driver is ultimately to be utilized in some flat response alignment, the distortion curves should be viewed in the perspective of flat acoustical output. A compressor or equalizer can be used to adjust the acoustic output of the driver to some constant sound pressure level with varying frequency down to the thermal or physical excursion limit of the unit. Fig. 9 shows the same driver of Fig. 8 adjusted for a constant 104.5-dB sound pressure level. If we compute the peak excursion for 3% distortion at this drive level,

$$x_{peak} = \frac{(1.18 \times 10^3) \, 10^{104/20}}{(60)^2 \, (167)^2} = 1.9 \text{ mm} \qquad (33)$$

showing better agreement with the prediction. It is important to note that this method will not change the frequency or shape of the resonance, so that possible changes in linearity may not be noticed.

Fig. 10 shows the response of another 380-mm driver with a progressive suspension and a heavier, stiffer cone than the previous unit, driven with 10 V rms (8 Ω nominal impedance). It is fitted with a 11.2-mm coil in a 7.2-mm gap, so that the predicted linearity is

$$x_{max} = \frac{11.2 - 7.2}{2} = 2.0 \text{ mm}. \qquad (34)$$

The 3% distortion point gives

$$x_{peak} = \frac{(1.18 \times 10^3) \, 10^{101.5/20}}{(52)^2 \, (167)^2} = 1.9 \text{ mm}. \qquad (35)$$

Fig. 11 shows the same unit equalized for 104.5-dB constant output. The third harmonic gives

$$x_{peak} = \frac{(1.18 \times 10^3) \, 10^{105/20}}{(57)^2 \, (167)^2} = 2.3 \text{ mm} \qquad (36)$$
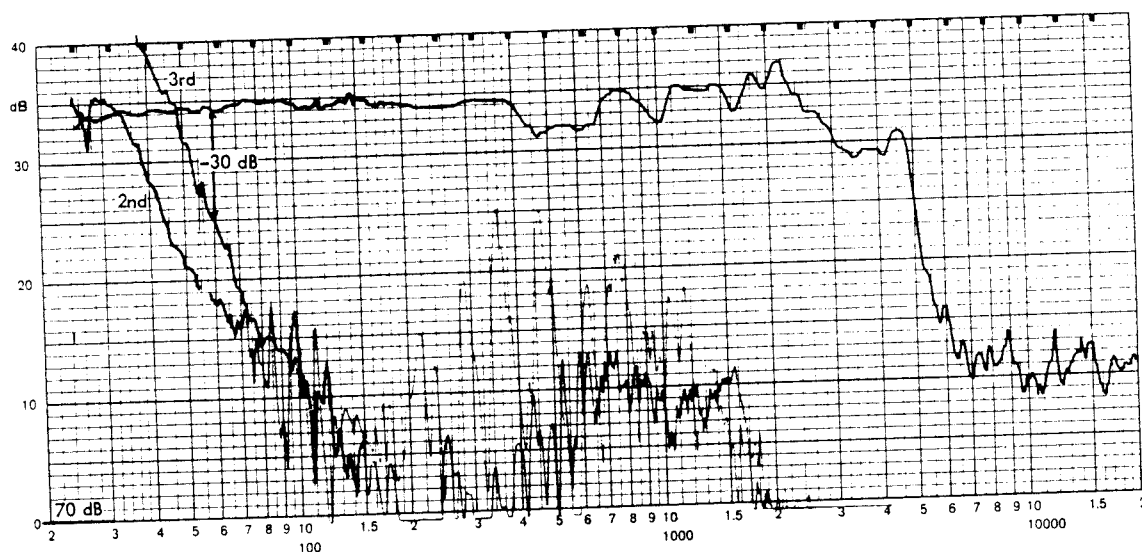
Fig. 9. Loudspeaker of Fig. 8 equalized for constant sound pressure level output. 45 V rms input at 30 Hz decreasing to 5 V rms at 400 Hz and above. Distortion products raised 20 dB.
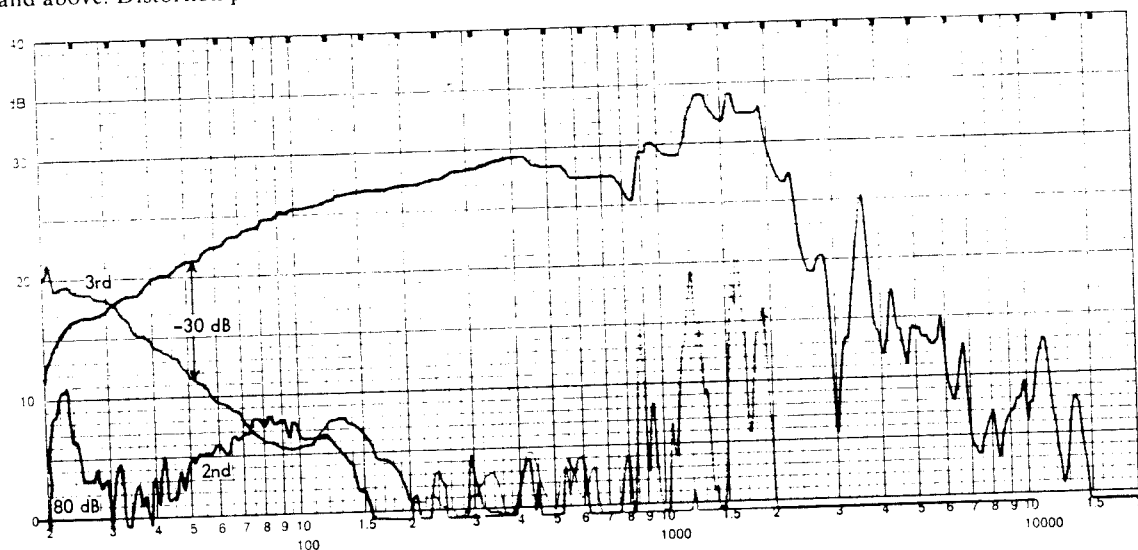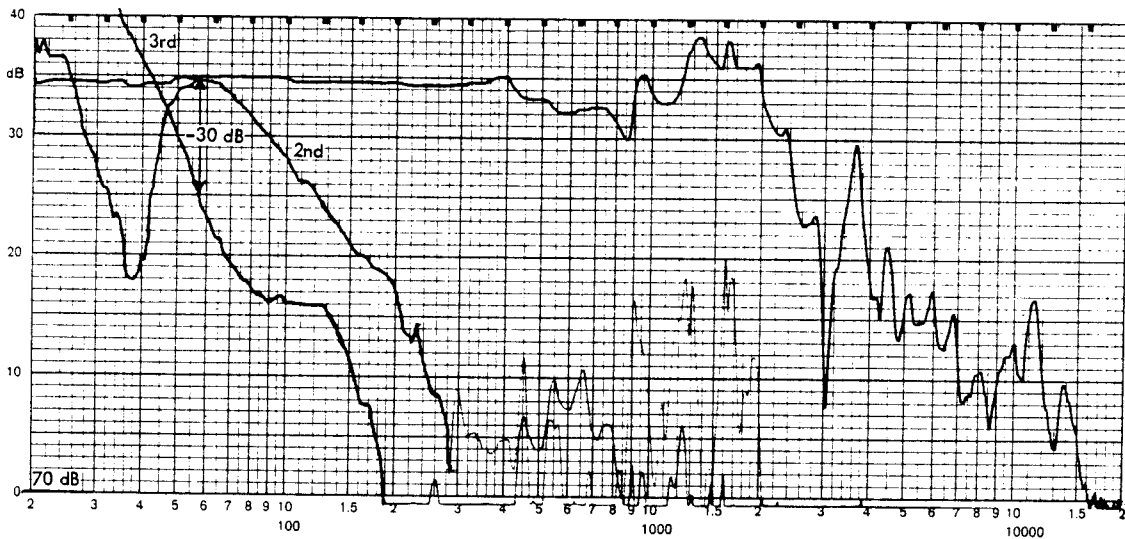

Fig. 10. Half-space on-axis response of a 380-mm (167-mm effective piston radius) loudspeaker with 11.2-mm coil in a 7.2-mm gap, 10 V rms input, 8 Ω nominal impedance. Distortion products raised 20 dB.

showing at this drive level some linearity increase due to the action of the progressive suspension. The second harmonic shows a large increase in the region from resonance, 38 Hz, on up to 200 Hz. The fact that the second harmonic drops at resonance indicates that this rise is probably the result of a dc shift in the coil rest position due to the magnetic rectification or coil jump-out effect. In this case the progressive suspension was sufficient to slightly increase linearity, but not strong enough to prevent the dc offset.

Fig. 12 shows the response of a 380-mm unit with the same 7.2-mm equal coil and gap motor of the unit in Fig. 6 fitted to the cone and progressive suspension of the unit in Figs. 8 and 9. The predicted linearity is again

$$x_{max} = \frac{7.2 - 7.2}{2} + 0.15\,(7.2) = 1.1 \text{ mm} \qquad (37)$$

and the third-harmonic 3% distortion point indicates

$$x_{peak} = \frac{(1.18 \times 10^3)\,10^{103/20}}{(72)^2\,(167)^2} = 1.2 \text{ mm}. \qquad (38)$$

In Fig. 13, at the higher voltages necessary to produce a constant 104-dB output,

$$x_{peak} = \frac{(1.18 \times 10^3)\,10^{104/20}}{(72)^2\,(167)^2} = 1.3 \text{ mm}. \qquad (39)$$

The linearity is slightly increased due to the progressive suspension.

Fig. 14 shows a long-excursion 380-mm unit fitted with a highly compliant foam surround, a fairly linear centering spider, and an underhung 7.2-mm coil in a 15.2-mm gap, at 20 V drive (8 Ω nominal impedance). The predicted linearity is

Fig. 11. Loudspeaker of Fig. 10 equalized for constant sound pressure level output. 30 V rms input at 20 Hz decreasing to 6 V rms at 400 Hz and above. Distortion products raised 20 dB. The action of the progressive suspension has increased linearity at higher drive, but is insufficient to prevent dc shift due to rectification, causing high second-harmonic distortion.
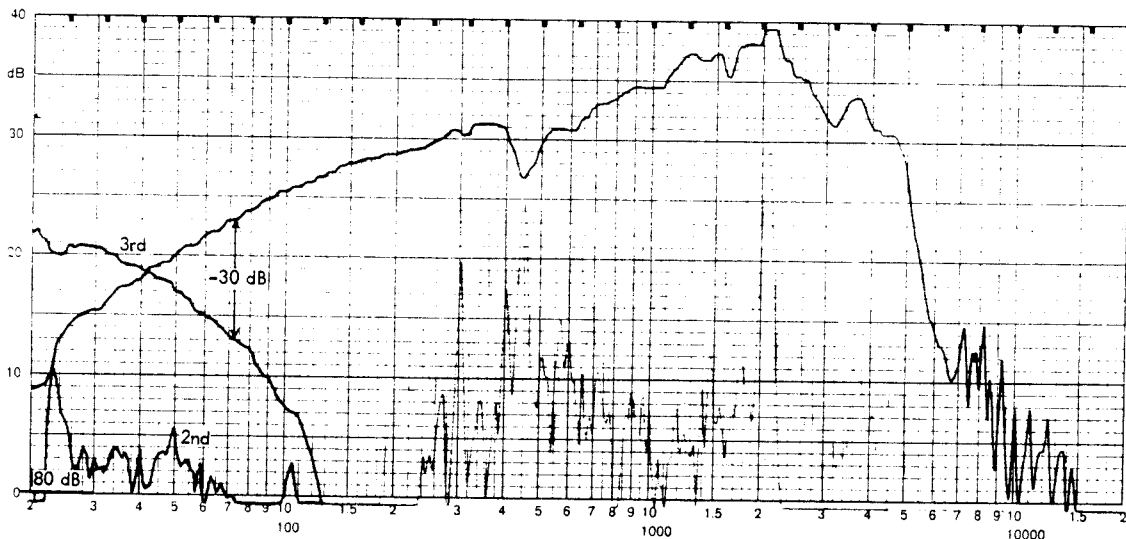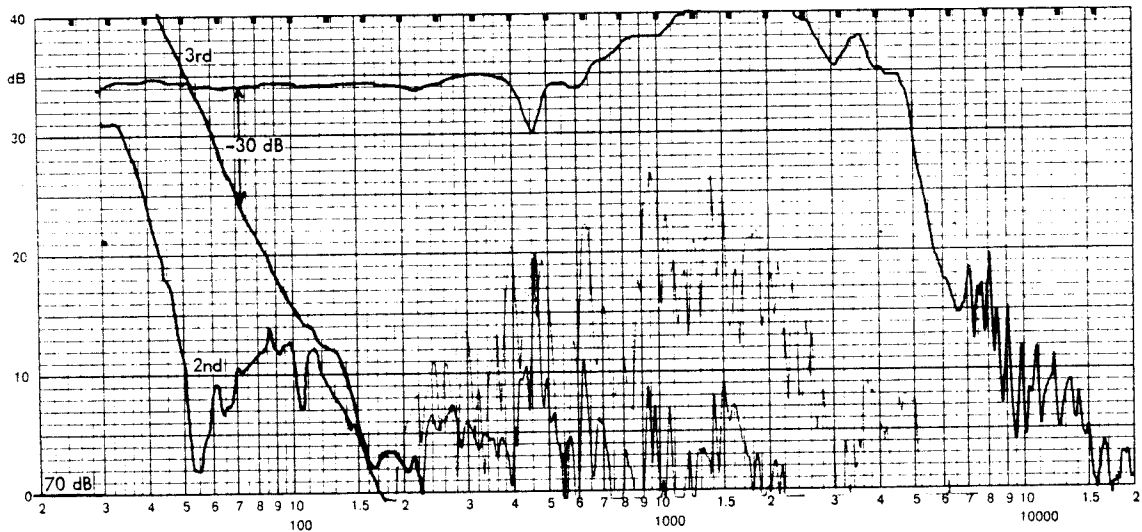

Fig. 12. Half-space on-axis response of a 380-mm (167-mm effective piston radius) loudspeaker with 7.2-mm equal coil and gap, 13 V rms input, 16 Ω nominal impedance. Distortion products raised 20 dB.

$$x_{max} = \frac{15.2 - 7.2}{2} + 0.15\,(7.2) = 5.1\ \text{mm} \qquad (40)$$

and the 3% third harmonic gives

$$x_{peak} = \frac{(1.18 \times 10^3)\,10^{107.5/20}}{(43)^2\,(167)^2} = 5.4\ \text{mm}. \qquad (41)$$

With the response equalized for 104.5-dB output (Fig. 15),

$$x_{peak} = \frac{(1.18 \times 10^3)\,10^{104.5/20}}{(37)^2\,(167)^2} = 5.2\ \text{mm}. \qquad (42)$$

Fig. 16 shows a different long-excursion 380-mm unit with the same high-compliance surround and spider, but with an overhung coil 15.8 mm long in a 7.2-mm gap at 20 V rms drive (8 Ω nominal impedance). The predicted

linearity is

$$x_{max} = \frac{15.8 - 7.2}{2} = 4.3\ \text{mm} \qquad (43)$$

and the 3% third-harmonic distortion point indicates

$$x_{peak} = \frac{(1.18 \times 10^3)\,10^{105.5/20}}{(43)^2\,(167)^2} = 4.3\ \text{mm}. \qquad (44)$$

In Fig. 17 at 104.5-dB constant output,

$$x_{peak} = \frac{(1.18 \times 10^3)\,10^{104.5/20}}{(41)^2\,(167)^2} = 4.2\ \text{mm}. \qquad (45)$$

If we look at this same driver at a constant 30-V rms, the offset rectification problem has manifested itself at this drive level from resonance, 36 Hz, up to 125 Hz,

Fig. 13. Loudspeaker of Fig. 12 equalized for constant sound pressure level output. 46 V rms input at 30 Hz decreasing to 6 V rms at 400 Hz and above. Distortion products raised 20 dB. At increased input, the linearity is increased due to the action of the progressive suspension.
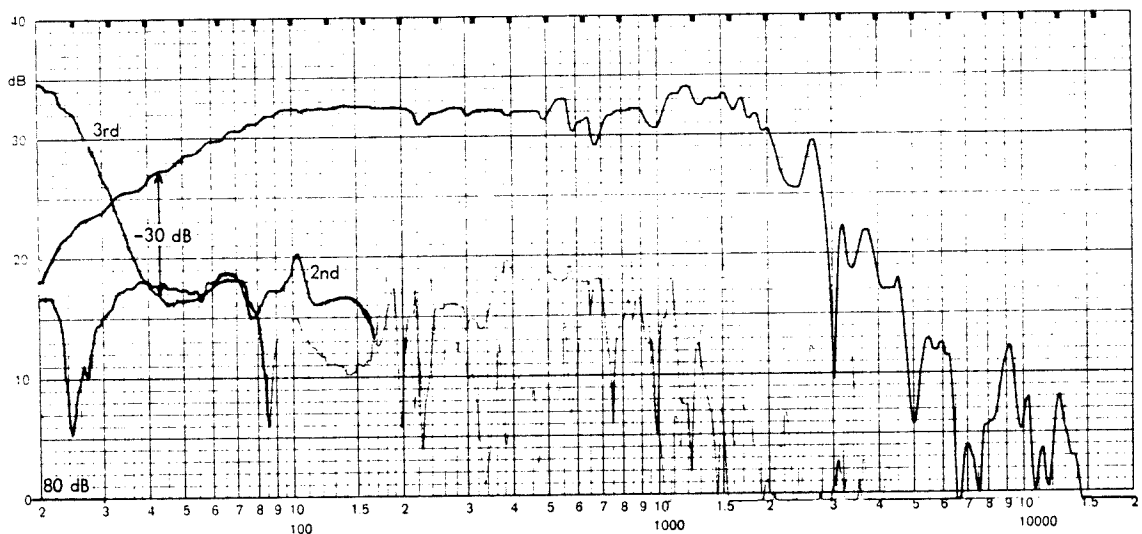

Fig. 14. Half-space on-axis response of a 380-mm (167-mm effective piston radius) loudspeaker with a 7.2-mm coil in a 15.2-mm gap, 20 V rms input, 8 Ω nominal impedance. Distortion products raised 20 dB.
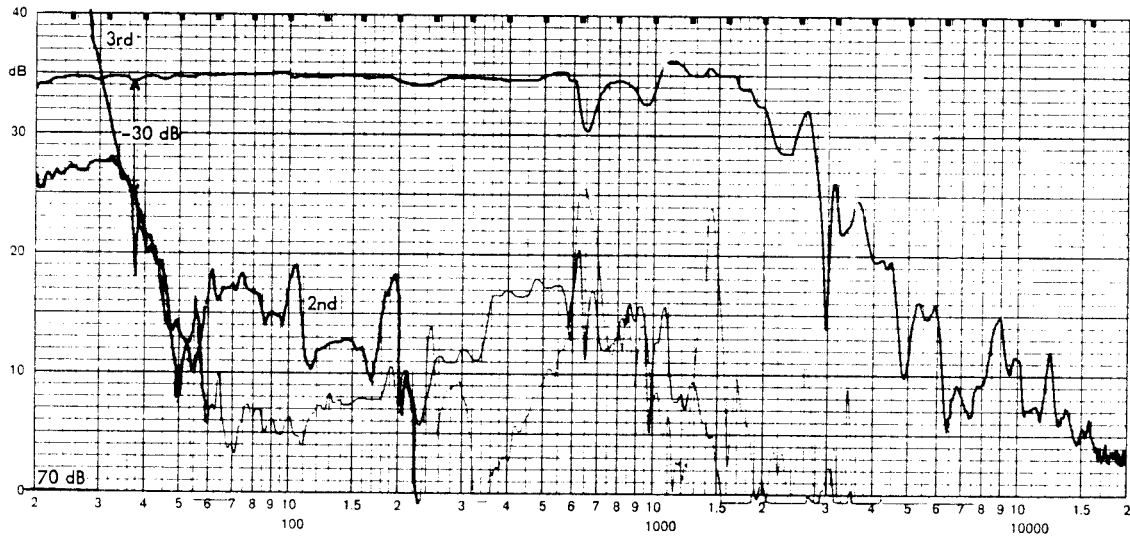
Fig. 15. Loudspeaker of Fig. 14 equalized for constant sound pressure level output. 28 V rms at 20 Hz decreasing to 8 V rms at 400 Hz and above. Distortion products raised 20 dB.
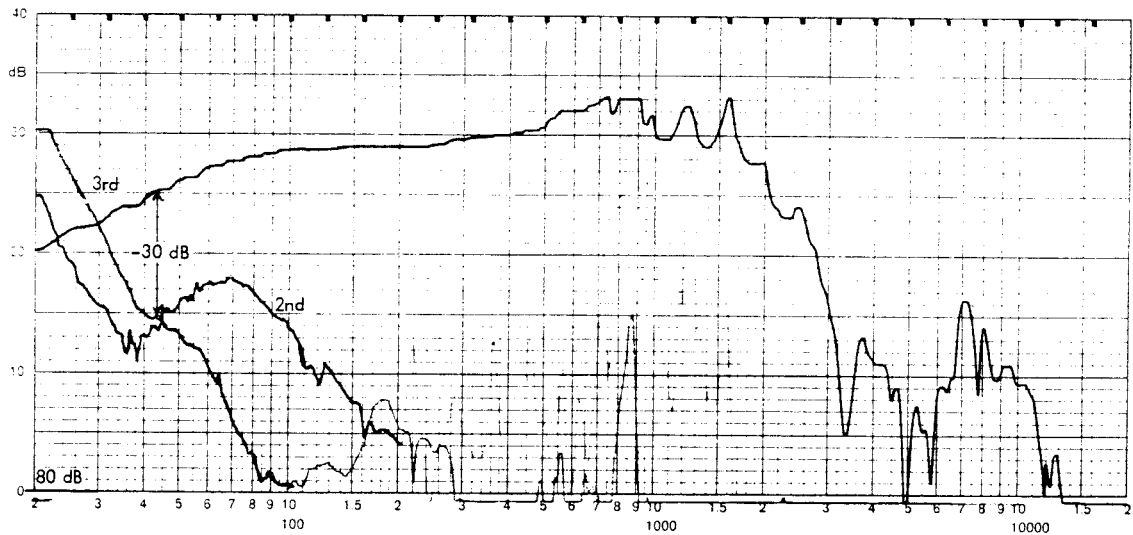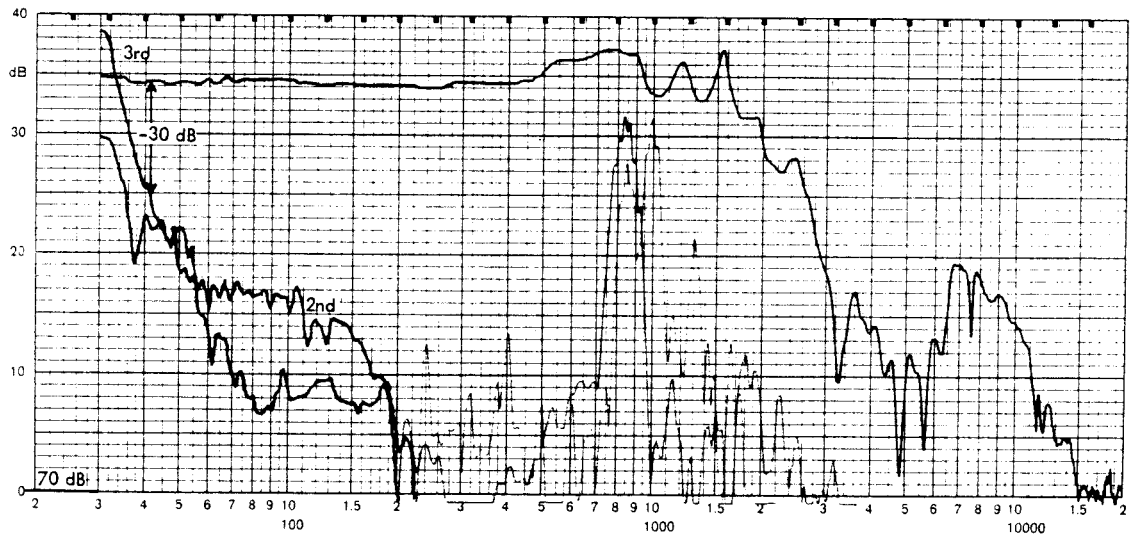

Fig. 16. Half-space on-axis response of a 380-mm (167-mm effective piston radius) loudspeaker with a 15.8-mm coil in a 7.2-mm gap, 20 V rms input, 8 Ω nominal impedance. Distortion products raised 20 dB.

Fig. 17. Loudspeaker of Fig. 16 equalized for constant sound pressure level output. 25 V rms at 30 Hz decreasing to 10 V rms at 400 Hz and above. Distortion products raised 20 dB.

giving high second-harmonic distortion over much of this region (Fig. 18).

Fig. 19 shows the same driver fitted with a progressive suspension. 3% third harmonic gives

$$x_{peak} = \frac{(1.18 \times 10^3) \, 10^{109.5/20}}{(54)^2 (167)^2} = 4.3 \text{ mm.} \qquad (46)$$

As predicted, the second harmonic remains low throughout. The offset has been prevented at no loss in total excursion linearity.

All of the previous examples have used 100-mm-diameter single-layer ribbon-wire coils in 1.5 mm wide symmetrical field geometry gaps. Fig. 20 shows a 250-mm (104-mm effective piston radius) driver with a two-layer roundwire 50-mm-diameter coil, 14.0 mm high, in a 5.7-mm gap, 1.2 mm wide, driven at 10 V (8 Ω nominal impedance). The prediction gives

$$x_{max} = \frac{14.0 - 5.7}{2} = 4.2 \text{ mm} \qquad (47)$$

and the curve shows 3% third-harmonic distortion at

$$x_{peak} = \frac{(1.18 \times 10^3) \, 10^{98.5/20}}{(48)^2 (104)^2} = 4.0 \text{ mm.} \qquad (48)$$

In this case a slight off-center placement of the rest position of the coil is responsible for the second harmonic reaching the same level as the third.

Fig. 21 shows a lower efficiency 250-mm unit with a 15.8-mm coil in an 8.1-mm gap. While the formula predicts

$$x_{max} = \frac{15.8 - 8.1}{2} = 3.9 \text{ mm} \qquad (49)$$

inspection of the unit reveals that the suspension limits are reached at approximately this excursion. The 3% third-harmonic distortion point indicates

$$x_{peak} = \frac{(1.18 \times 10^3) \, 10^{95/20}}{(28)^2 (103)^2} = 8 \text{ mm} \qquad (50)$$
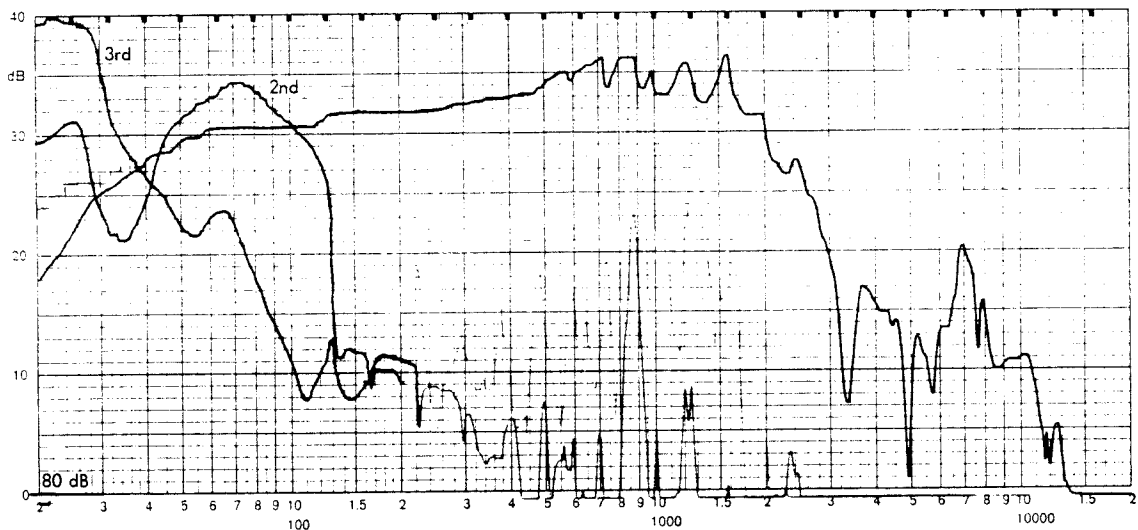

Fig. 18. Loudspeaker of Fig. 16 at 30 V rms input. Distortion products raised 20 dB. Rectification effects causing large dc offset and increased distortion from resonance, 36 Hz, up to 125 Hz.
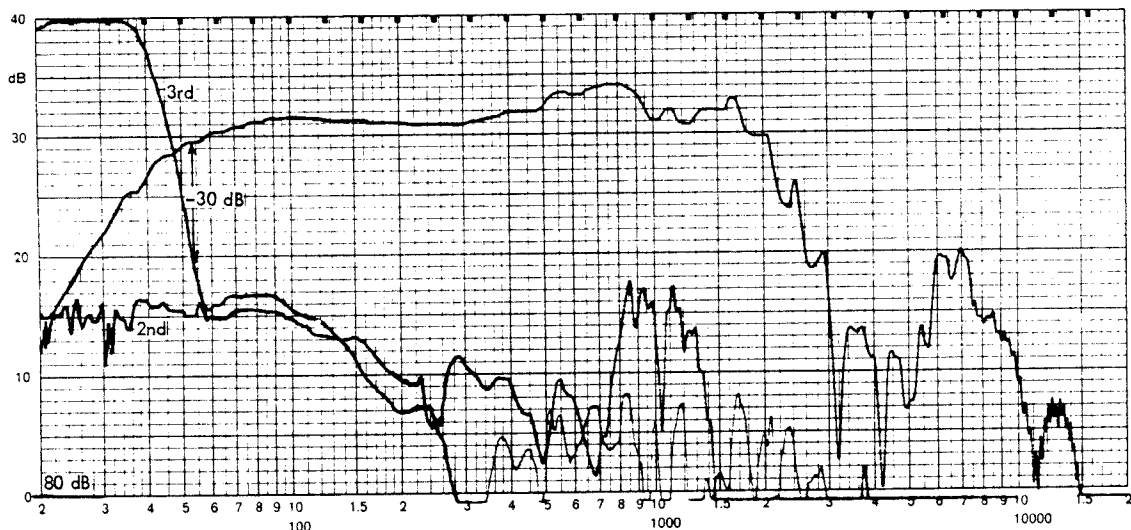

Fig. 19. Same type of loudspeaker as in Fig. 1B fitted with progressive suspension, 30 V rms input. Distortion products raised 20 dB. Suspension has prevented dc offset and allowed linearity to reach the full potential of the motor topology.

which means that one end of the coil has moved halfway through the gap before the distortion rises significantly. Here we have a case where at the extremes of coil and cone motion, the nonlinearities of the motor are balanced by those of the suspension, yielding increased total linearity (resonance was at 30 Hz). Unfortunately this unit has a severe flux modulation problem, as evidenced by the relatively constant high level of second-harmonic distortion from resonance all the way out to 600 Hz. The unit is also constructed with nonsymmetrical field geometry, which together with miscentering is responsible for the second harmonic also being higher than the third below resonance.

Fig. 22 shows a 300-mm unit with symmetrical field geometry, but with a similar flux modulation problem.

Fig. 23 shows the same type of structure, but assembled with an aluminum ring around the bottom of the center pole support acting as a shorted turn to stabil-

ize the flux, preventing modulation. The second-harmonic components in the midband have been reduced more than 20 dB.

Fig. 24 shows a 460-mm unit (184-mm effective piston radius) with a 19.1-mm-long coil in an 8.9-mm gap. This unit is fitted with a one-piece paper cone with a treated edge compliance, and while we would predict

$$x_{max} = \frac{19.1 - 8.9}{2} = 5.1 \text{ mm} \tag{51}$$

the curve shows

$$x_{peak} = \frac{(1.18 \times 10^3) \, 10^{116/20}}{(87)^2 \, (184)^2} = 2.9 \text{ mm}. \tag{52}$$

In this case the surround is too stiff, too progressive, and limits the linearity potential of the motor. A new cone
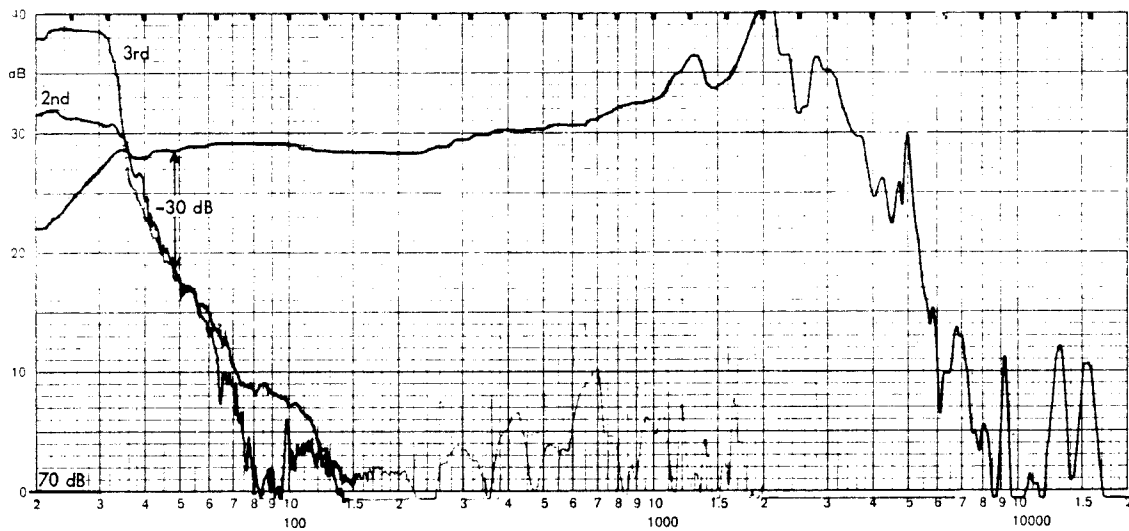

Fig. 20. Half-space on-axis response of a 250-mm (104-mm effective piston radius) loudspeaker with a 14.0-mm coil in a 5.7-mm gap, 10 V rms input, 8 Ω nominal impedance. Distortion products raised 20 dB.
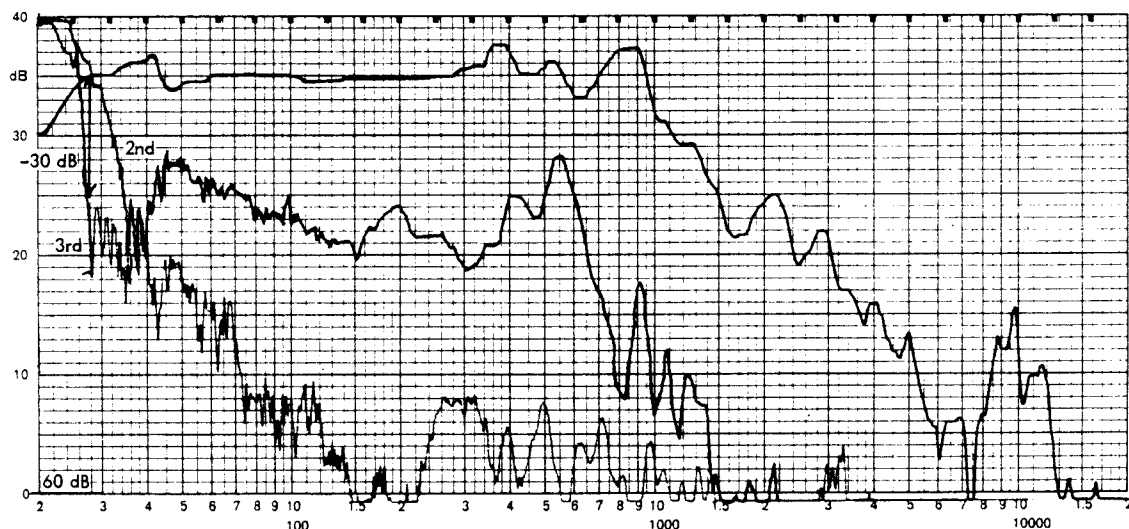

Fig. 21. Half-space on-axis response of a 250-mm (103-mm effective piston radius) loudspeaker with a 15.8-mm in an 8.1-mm gap, 10 V rms input, 8 Ω nominal impedance. Distortion products raised 20 dB. Unit has nonsymmetrical gap geometry and exhibits flux modulation distortion, causing high second-harmonic distortion.
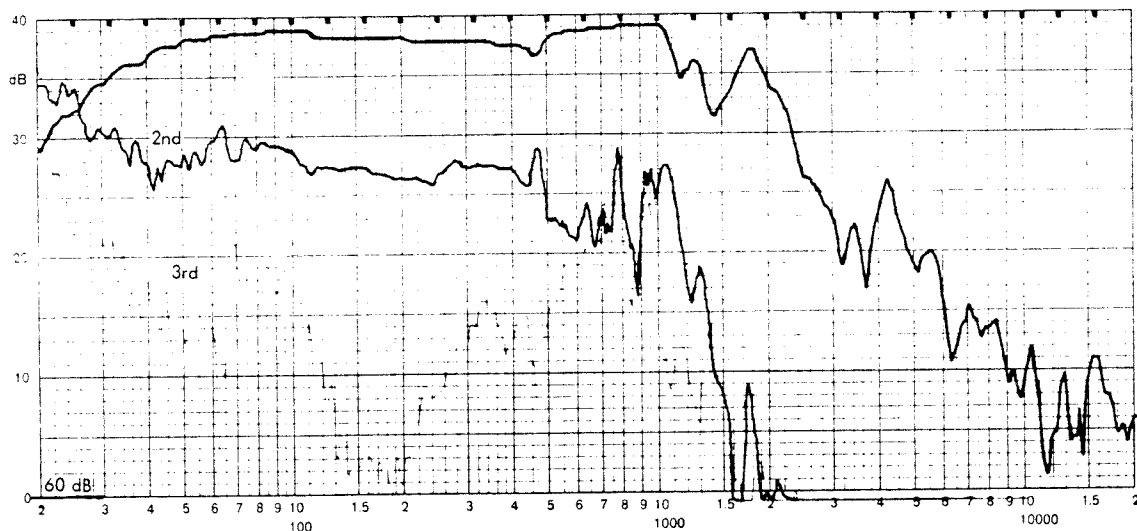
Fig. 22. 300-mm loudspeaker at 9 V input, 8 Ω nominal impedance. Distortion products raised 20 dB. Unit exhibits flux modulation distortion.
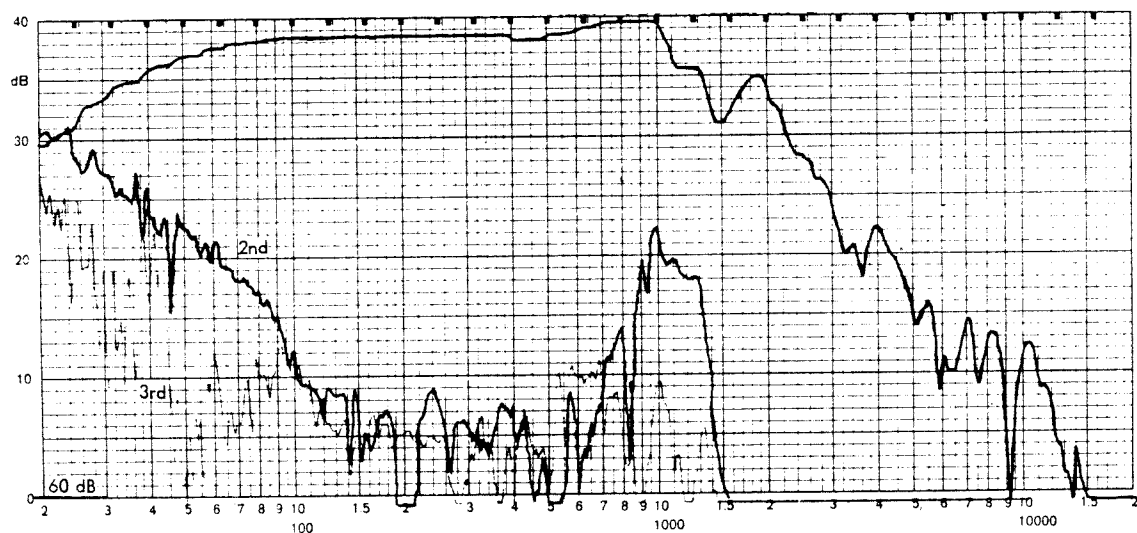

Fig. 23. Same type of loudspeaker as in Fig. 22, but with conductive ring within magnet structure eliminating flux modulation. 9 V input, 8 Ω nominal impedance. Distortion products raised 20 dB. Midband second-harmonic distortion has been reduced 20 dB through the action of the ring.
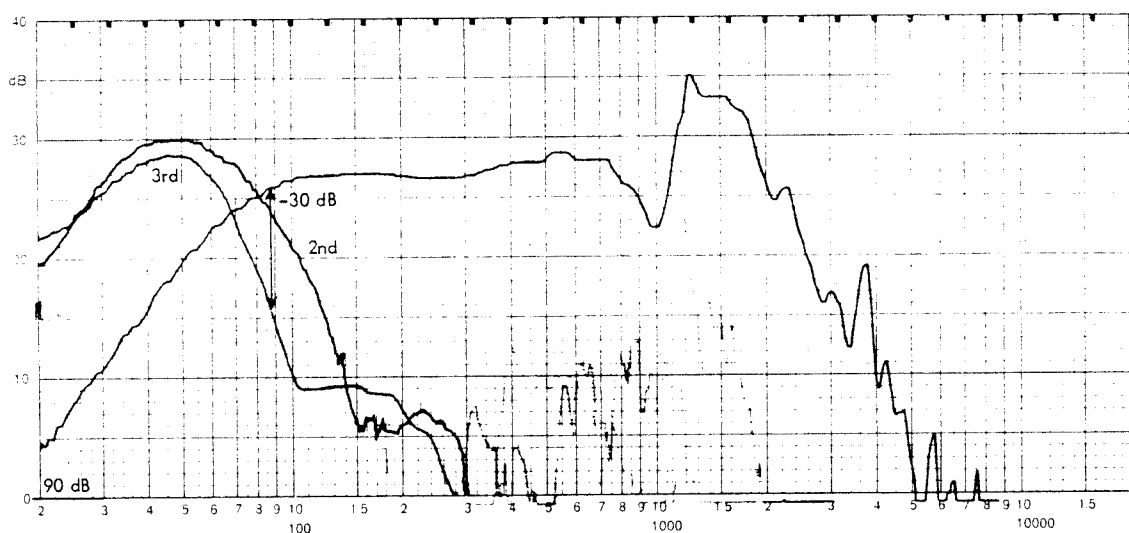

Fig. 24. 460-mm loudspeaker at 30 V input, 8 Ω nominal impedance. Distortion products raised 20 dB. Excessive surround stiffness limits potential motor linearity.

and surround were fitted and the results (Fig. 25) show that a better balance of forces has been achieved:

$$x_{peak} = \frac{(1.18 \times 10^3) \, 10^{116/20}}{(67)^2 \, (184)^2} = 4.9 \text{ mm}. \tag{53}$$

12 SUMMARY AND CONCLUSIONS

The peak displacement limit of a moving-coil loudspeaker can be approximately predicted by the amount of voice-coil overhang for long coil–short gap structures, and by the amount of voice-coil underhang plus a 15% increase due to the fringe field for underhung and equal coil and gap units. This will predict the excursion for 3% third-harmonic distortion. This can be extended in cases where the suspension force compensates for nonlinear motor force, or degraded where the suspension force increases at too fast a rate. Second-harmonic distortion can arise from a number of sources, all of which place the rest position of the coil away from the position of maximum Bl. These factors all apply to motor geometry, which is the dominant distortion mechanism below approximately 150 Hz for low-frequency drivers. In the region up to the piston band limit, motor structure nonlinearities such as air venting, magnetization, and flux modulation are the dominant distortion mechanisms. Above the piston band limit, cone breakup is the dominant nonlinearity. The peak displacement for a moving-coil direct-radiator loudspeaker operating in the piston band can be derived directly from acoustic pressure measurements.

13 ACKNOWLEDGMENT

14 REFERENCES

[1] L. L. Beranek, *Acoustics* (McGraw-Hill, New York, 1954).

[2] L. E. Kinsler and A. R. Frey, *Fundamentals of Acoustics*, 2nd ed. (Wiley, New York, 1962).

[3] A. N. Thiele, "Loudspeakers In Vented Boxes: Part II," *J. Audio Eng. Soc.*, vol. 20, pp. 471–483 (1971 June).

[4] R. H. Small, "Direct-Radiator Loudspeaker System Analysis," *J. Audio Eng. Soc.*, vol. 20, pp. 383–395 (1972 June).

[5] R. H. Small, "Closed-Box Loudspeaker Systems: Part I: Analysis," *J. Audio Eng. Soc.*, vol. 20, pp. 798–808 (1972 Dec.).

[6] H. F. Olson, "Analysis of the Effects of Nonlinear Elements upon the Performance of a Back-Enclosed, Direct Radiator Loudspeaker Mechanism," *J. Audio Eng. Soc.*, vol. 10, pp. 156–162 (1962 Apr.).

[7] N. W. McLachlan, *Loudspeakers: Theory, Performances Testing and Design*, corrected ed. (Dover, New York, 1960).

[8] W. J. Cunningham, "Non-Linear Distortion in Dynamic Loudspeakers Due to Magnetic Effects," *J. Acoust. Soc. Am.*, vol. 21, pp. 202–207 (1949 May).

[9] D. Hermans, "Low Frequency Distortion in Loudspeakers," presented at the 56th Convention of the Audio Engineering Society, Paris, 1977 Mar. 1–4.

[10] D. A. Barlow, "Instability in Moving Coil Loudspeakers," presented at the 50th Convention of the Audio Engineering Society, London, 1975 Mar. 4–7.

[11] H. D. Harwood, "Loudspeaker Distortion Associated with Low-Frequency Signals," *J. Audio Eng. Soc.*, vol. 20, pp. 718–728 (1972 Nov.).

[12] H. F. Olson, "The Action of a Direct Radiator Loudspeaker with a Non-Linear Cone Suspension System," *J. Acoust. Soc. Am.*, vol. 16, pp. 1–4 (1944 July).

[13] T. H. Wiik, "Transient Distortion Caused by Nonlinearities in Driving Force and Suspension of a Loudspeaker," presented at the 56th Convention of the Audio Engineering Society, Paris, 1977 Mar. 1–4, preprint 1205.

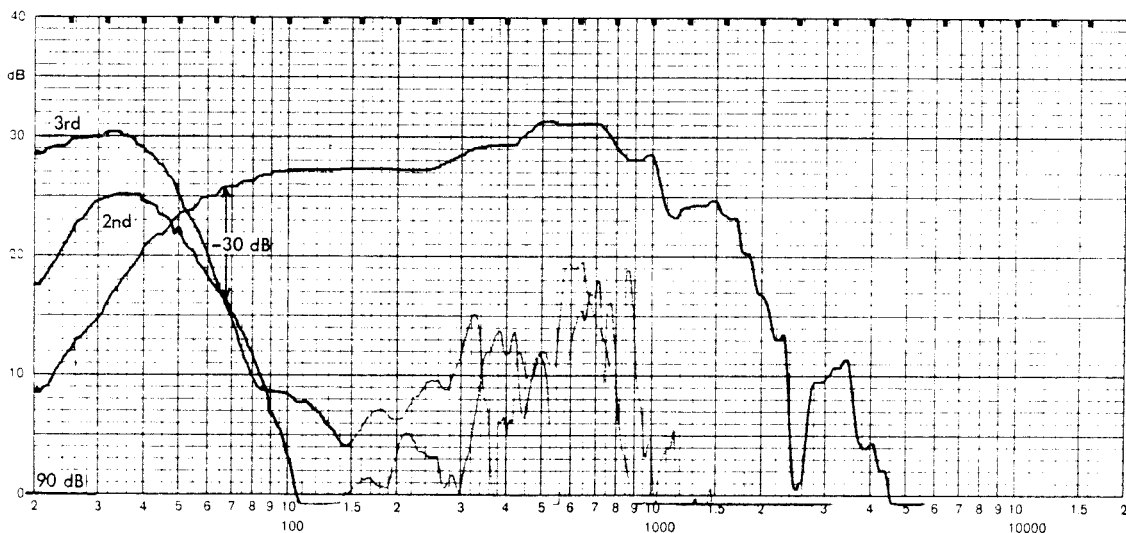[14] J. R. Gilliom, "Distortion in Dynamic Loud-

Fig. 25. Loudspeaker of Fig. 24 fitted with more linear sound. 30 V input, 8 Ω nominal impedance. Distortion products raised 20 dB.

speakers Due to Modulation of the Permanent Field," presented at the 42nd Convention of the Audio Engineering Society, Los Angeles, 1972 May 2–5.

[15] J. R. Gilliom, B. L. Boliver, and L. C. Boliver "Design Problems of High-Level Cone Loudspeakers," *J. Audio Eng. Soc., (Project Notes/Engineering Briefs)*, vol. 25, pp. 294–299 (1977 May).

[16] J. King, "Loudspeaker Voice Coils," *J. Audio Eng. Soc.*, vol. 18, pp. 34–43 (1970 Feb).

[17] R. H. Small, "Assessment of Non-linearity in Loudspeaker Motors," presented at the Convention of IREE, Australia, 1979 Sept.

[18] J. E. Weaver and W. M. Leach, Jr., "Optimal Measurement of Loudspeaker Driver Large Signal Displacement," *J. Audio Eng. Soc.*, vol. 26, pp. 145–148 (1978 Mar.).

[19] J. Christophorou, "Low Frequency Loudspeaker Measurements with an Accelerometer," *J. Audio Eng. Soc.*, vol. 28, pp. 809–817 (1980 Nov.).

[20] D. B. Keele, Jr., "Low-Frequency Loudspeaker Assessment by Nearfield Sound-Pressure Measurements," *J. Audio Eng. Soc.*, vol. 22, pp. 154–162 (1974 Apr.).

THE AUTHOR

Mark R. Gander was born in New Brunswick, New Jersey in 1952. Prior to college he received an extensive musical education. He later earned a B.S. degree from Syracuse University in 1974, and worked as a sound engineer and audio systems designer in broadcasting, studio recording, and concert reinforcement.

In 1976 he received an M.S.E.E. from The Georgia Institute of Technology, specializing in audio electronics and instrumentation, including the multidisciplinary program in acoustical engineering. That same year he joined James B. Lansing Sound, Inc. as a transducer engineer where he had design responsibility for various consumer and professional loudspeaker products, including the Cabaret Series and E Series musical instrument loudspeakers. Since 1980 he has been an applications engineer for the JBL Professional Division.

Mr. Gander's articles have been published in the *Journal of the Audio Engineering Society*, *dB Magazine*, *Sound Arts*, and *Modern Recording*. He holds an FCC First Class Radiotelephone Operator License, and is a member of the AES, The Acoustical Society of America, and the IEEE.